Int. J. Electrochem. Sci., 13**(2018)** 10415 – 10426, doi: 10.20964/2018.11.45

International Journal of ELECTROCHEMICAL SCIENCE
www.electrochemsci.org

Determination of Lead(II) Using Glassy Carbon Electrode Modified with Hexagonal Co_3O_4 Microparticles

Jingmin Liu, Riya Jin[*]*, YinaQiao, Yuanyuan Wu, Xiaojian Wang, Ying Wang*

School of Environment and Safety Engineering, North University of China, Taiyuan, Shanxi 030051, People's Republic of China.
[*]E-mail:jrya@nuc.edu.cn

Received: 8 July 2018/ *Accepted:* 28 August 2018 / *Published:* 1 October 2018

In this study, cobaltosic oxide (Co_3O_4) was synthesized by a simple surfactant-free hydrothermal method. The as-prepared materials were characterized by scanning electron microscope and X-ray diffraction, indicating that Co_3O_4 is formed by stacked hexagonal microsheets. The as-obtained microsheet-stacked Co_3O_4 was drop-coated on glassy carbon electrode (GCE) to allow the fabrication of electrochemical sensors for the detection of trace Pb^{2+} by square wave anodic stripping voltammetry. The proposed Co_3O_4/GCE sensors exhibited a linear correlation for Pb^{2+} concentration in the concentration range from 0.5 to 5 μM, and the limit of detection was calculated as 1.18×10^{-8} M (S/N=3). The results showed that the as-prepared Co_3O_4/GCE sensor had good repeatability and sensitivity and the ability to effectively avoid the interference from Cd^{2+} and Hg^{2+}. In addition, the method for the preparation of proposed sensor was simple and cost effective. Overall, this work provides a promising material for electrochemical detection of heavy metal ions in water.

Keywords: Hydrothermal; Co_3O_4; Square wave anodic stripping voltammetry (SWASV); Lead(II)

1. INTRODUCTION

Lead is a toxic heavy metal. With the rapid development of the industrial market, lead has been widely used in all walks of life. Lead and its compounds even in small concentrations can damage multiple systems such as the brain, nerves, digestion, and kidneys [1–4]. Currently, most commonly used analytical procedures for the determination of lead(II) (Pb^{2+}) are based on atomic absorption spectrometry [5–7], atomic fluorescence spectrometry [8,9], inductively coupled plasma mass spectrometry [10–12], ion chromatography [13], X ray fluorescence spectrometry [14], spectrophotometry [15,16]. Although these methods are sufficiently sensitive, they are time-consuming, expensive, require complex pre-processing procedures and professional operators, and can only be used indoor. Hence, it is highly fascinating to find a rapid, accurate, and simple analytical

technique to detect Pb^{2+}. Considering electrochemical technology has the advantages of high sensitivity, real-time on-line analysis, low cost, and simple pre-treatment [1,4,17,18], a chemically modified electrode was designed for the detection of Pb^{2+} in water.

Cobaltosic oxide (Co_3O_4) with AB_2O_4 spinel structure is a significant magnetic *p*-type semiconductor oxide [19]. Co_3O_4 is widely used in sensors, supercapacitors, lithium-ion batteries, catalytic materials, and magnetic materials owing to its magnetism, diffusivity, conductivity, chemical activity, and catalysis [19–21]. A variety of methods including pyrolysis, chemical vapor deposition, pulsed laser deposition, and traditional sol-gel method have been used for preparing Co_3O_4 [22]. In the charge storage process, because of the difference in the material/electrolyte interface properties and ion transfer rate, Co_3O_4 of different surface morphologies showed marked differences in their electrochemical properties [23,24]. Liu synthesized Co_3O_4 microspheres through a simple hydrothermal treatment [25], exhibiting good electrochemical behaviors as lithium ion anode materials. Xie successfully synthesized layered Co_3O_4 consisting of oriented and self-assembled micrometer-length rectangular 2D flakes by a hydrothermal method followed by the subsequent calcination process [23]. The as-prepared Co_3O_4 sample provides a potential electroactive material for supercapacitor. Zhang described hierarchical Co_3O_4 nanoporous nanoflowers prepared via a hydrothermal reaction followed by heat treatment [26]. The main anti-ferromagnetic property of Co_3O_4 nanoflowers was exhibited by temperature dependence curve of magnetization in zero-field-cooled, while the weak ferromagnetic characteristics of Co_3O_4 nanoflowers can be shown from temperature dependence curve of magnetization in field-cooled. Wen successfully prepared rhombus-shaped Co_3O_4 nanorod (NR) arrays through a fluorine-mediated hydrothermal method [27]. The prepared Co_3O_4 was used as an ethanol sensor material, exhibiting good performance for ethanol detection.

In this study, a surfactant-free simple hydrothermal method was used to obtain Co_3O_4 of hexagonal structure with special morphology and uniformity in a reasonable reaction time and temperature. A highly sensitive sensor, Co_3O_4 modified glassy carbon electrode (GCE) abbreviated as Co_3O_4/GCE, was developed to detect trace Pb^{2+} by square wave anodic stripping voltammetry (SWASV). The anti-interference and repeatability of Co_3O_4/GCE are discussed in detail, and the as-prepared Co_3O_4/GCE was applied to real water sample analysis to demonstrate its practical application.

2. EXPERIMENTAL SECTION

2.1 Materials and Instruments

The material used in this study are as follows: Cobalt nitrate ($Co(NO_3)_2 \cdot 6H_2O$, Tianjin Hedong Hongyan Reagent Factory); Urea ($CO(NH_2)_2$, Tianjin BeichenFangzheng Reagent Factory); Ammonium fluoride (NH_4F, Tianjin Dengfeng Chemical Reagent Factory); Lead nitrate ($Pb(NO_3)_2$, Tianjin Guangfu Fine Chemical Research Institute). All the above reagents were of analytical grade and used without further purification unless otherwise noted. Ultrapure water with a resistance of 18.25 MΩ·cm was used for all the experiments.

The equipment used are as follows: Electrochemical workstation (CHI660E, Shanghai Chenhua Instrument Company); Three-electrode system: GCE, platinum electrode and saturated calomel electrode (SCE); Vacuum/atmosphere tubular resistance furnace 1200°C (TianjinLaiboTerui Instrument Equipment Co. Ltd.); Scanning electron microscope (JEOL Ltd.); X-ray diffractometer (Ultima IV, Dandong Haoyuan Instrument Co. Ltd.).

2.2 Synthesis of Co_3O_4

Co_3O_4 was prepared via the hydrothermal method without using any surfactant. The specific preparation process is as follows: 2 mmol $Co(NO_3)_2 \cdot 6H_2O$, 8 mmol NH_4F and 15 mmol $CO(NH_2)_2$ were dissolved in 40 mL of ultrapure water and stirred magnetically for 30 min at room temperature to make a homogeneous and transparent solution. Then, the mixed solution was transferred into a 50 mL Teflon-lined stainless steel autoclave. The autoclave was placed in an oven and reacted for 12 h at 110°C. After cooling down to room temperature, the pink-violet samples were collected by centrifugation. The samples were washed several times with anhydrous ethanol and ultrapure water successively and dried in a thermostatic drying oven at 80℃ for 10 h. Then, the samples were placed in a tube muffle furnace. The black Co_3O_4 powder was obtained by calcination at 400℃ for 3 h at a heating rate of 1℃/min.

2.3 Preparation of Co_3O_4/GCE

Before modification, the GCE was polished to a glossy surface with 0.05 μm alumina powder. The polished GCE was rinsed with ultrapure water, then ultrasonically washed in absolute ethanol and ultrapure water for 3 to 5 min, and finally dried under nitrogen atmosphere. Subsequently, 5 mg Co_3O_4 was dispersed in 5 mL water and kept in an ultrasonic bath for 10 min to make a homogeneous suspension. 10 μL of the suspension was taken with a pipette and dropped onto the surface of GCE, and the suspension was allowed to dry at room temperature to get Co_3O_4/GCE.

2.4 Electrochemical Measurements

The electrochemical behavior of Co_3O_4/GCE was observed by SWASV. First, Pb was deposited via the reduction of Pb^{2+} in supporting electrolyte with constant stirring. The parameters such as supporting electrolyte, deposition potential, and deposition time were individually optimized through experiments. Second, the anodic stripping (reoxidation of Pb to Pb^{2+}) was carried out in the potential range from −1.0 to 0 V under the following conditions: increment potential, 4 mV; amplitude, 25 mV; frequency, 15 Hz vs. SCE. At last, to avoid the remaining Pb^{2+} of the electrode affecting the experimental results, amperometric i–t curve was used for desorption. Under continuous stirring, desorption of Co_3O_4/GCE was completed at a potential of 0.2 V in 270 s. All the tests were performed at room temperature in the air.

3. RESULTS AND DISCUSSION

3.1 Morphology and Structure Characterization of Co_3O_4 Materials

The morphology and the structure of prepared Co_3O_4 samples were characterized by scanning electron microscope (SEM) and X-ray diffraction (XRD), respectively. Figure 1 shows the SEM images of Co_3O_4. Figures 1A and Figure 1B are the images of an uncalcined precursor, which was a particle stacked by hexagonal microsheets with a uniform particle size of 8 μm. The flake surface was smooth and the edge was scaly, which could provide a certain adsorption site for Pb^{2+} [28,29]. Figures 1C and Figure 1D are the images of the calcined product. Figure 1C shows that the particle size of the calcined product was slightly smaller than the precursor. The image was magnified up to 20,000 times (Figure 1D), clearly indicating that the precursor was completely oxidized by oxygen in the air at a high temperature of 400℃. The flake surface had a foam-like mesoporous characteristic, which could improve the specific surface area of the material and provide more adsorption sites for Pb^{2+}.

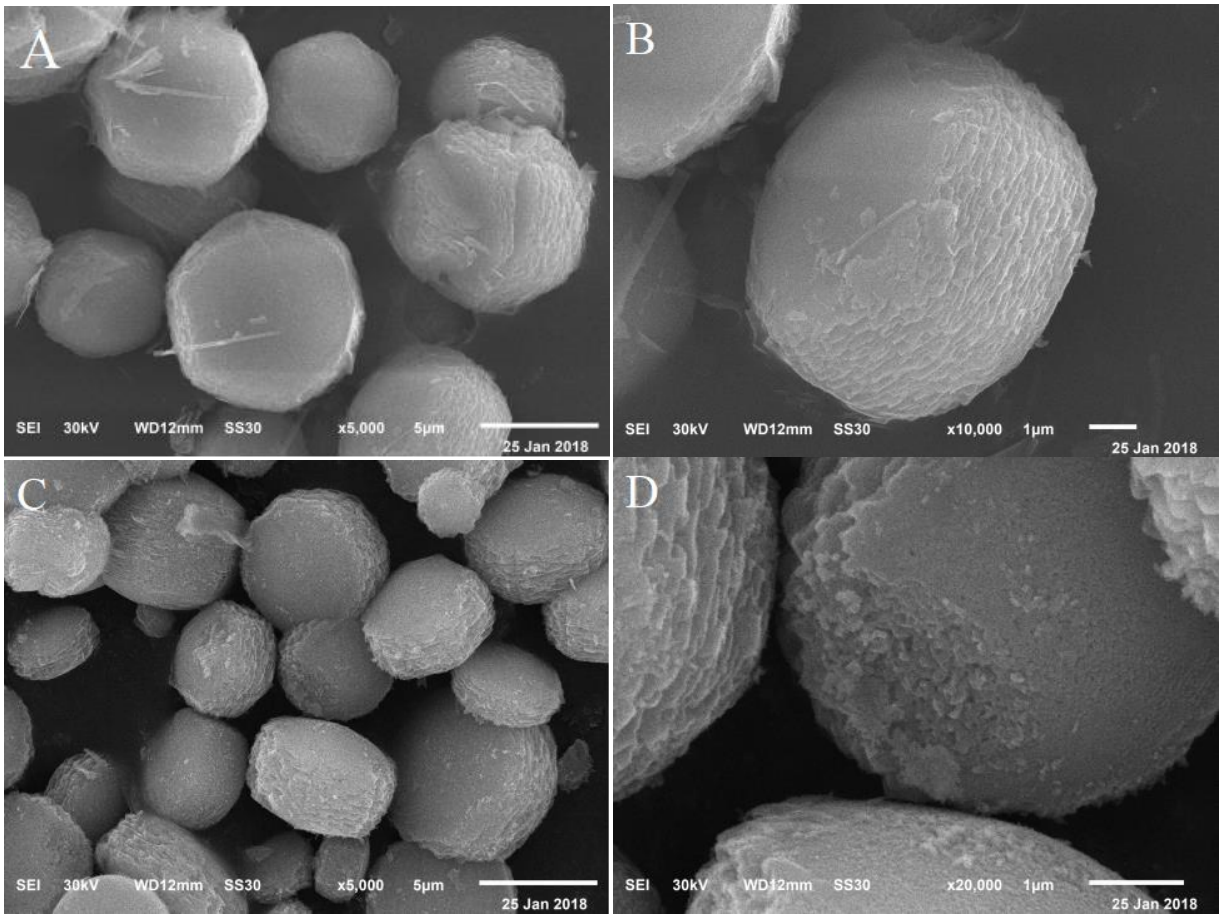

Figure 1. SEM images of Co_3O_4 precursors at magnifications of 5000 (A) and 10000 (B). SEM images of Co_3O_4 at magnifications of 5000 (C) and 20000 (D).

From Figure 2, we could infer the possible growth process of a single Co_3O_4 ultrafine particle. First, rod-like microwires grew on the surface of cobalt. And then, the microwires gradually stacked

into irregular microsheets. Further, irregular microsheets gradually grew into regular single-layer hexagonal microsheets. Finally, the single-layer hexagonal microsheets stacked into independent microsheets. Because of small crystallite size, large specific surface area, and porosity, the prepared Co_3O_4 had potential applications as electrochemical sensors and thus providing active centers for the accumulation of metal ions.

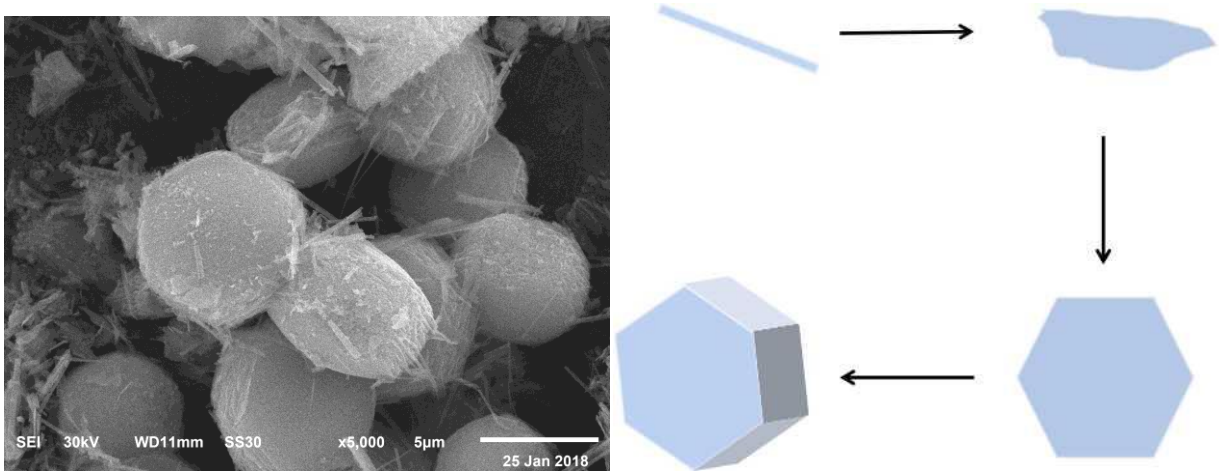

Figure 2. Schematic diagram of the growth process of hexagonal Co_3O_4 microparticles

Figure 3 shows the XRD pattern of the as-prepared Co_3O_4, indicating good crystallinity of the material. The diffraction peaks at the 2θ of 19°, 31.27°, 36.85°, 38.54°, 44.81°, 55.66°, 59.36° and 65.24° were consisitent with the diffractions of the crystal planes {111}, {220}, {311}, {222}, {400}, {422}, {511}, and {440} of the XRD of standard, respectively, and is in accordance with the literature values (JCPDS card No. 42-1467) [30]. These results indicated that Co_3O_4 has a pure spinel structure.

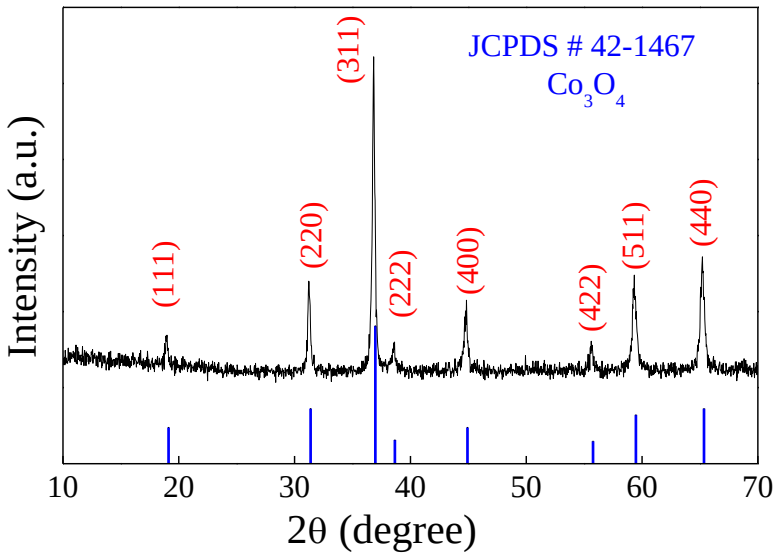

Figure 3. XRD pattern of the as-prepared microsheet-stacked Co_3O_4.

3.2 Electrochemical Characterization of Co_3O_4/GCE

Figure 4 shows the typical cyclic voltammetry (CV) response of GCE and Co_3O_4/GCE. Compared to GCE, the peak current of the oxidation and reduction peaks of Co_3O_4/GCE decreased. The decrease in the peak current could be attributed to successful modification of Co_3O_4 on the GCE surface. Moreover, the potential difference between the oxidation peak and the reduction peak was also larger than that of GCE, hindering the electron transfer on the electrode surface to a certain extent [29]. The peak current ratio of oxidation and reduction peak of Co_3O_4/GCE was close to 1, indicating that Co_3O_4/GCE had a good redox potential.

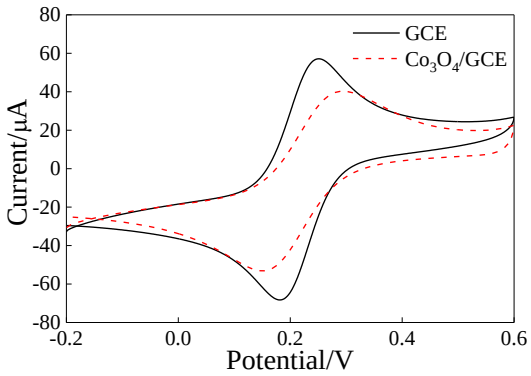

Figure 4. Cyclic voltammograms of GCE and Co_3O_4/GCE in 5.0 mM $[Fe(CN)_6]^{3-/4-}$ containing 0.1 M KCl. The potential range of CV is from –0.2 V to 0.6 V at a scan rate of 100 mV/s.

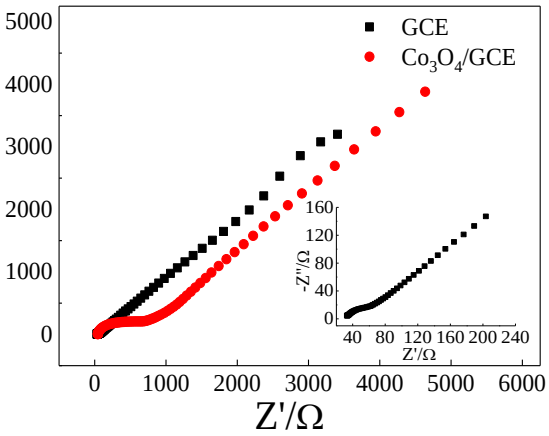

Figure 5. Electrochemical impedance plots of GCE and Co_3O_4/GCE in 5.0 mM $[Fe(CN)_6]^{3-/4-}$ containing 0.1 M KCl. The frequency range of EIS is 10 mHz–100 kHz.The amplitude is 5 mV, and the initial potential is 0.23 V.

Figure 5 shows the electrochemical impedance spectroscopy (EIS) of GCE and Co_3O_4/GCE. EIS is composed of two parts, high-frequency area and low-frequency area. The semicircle part of the high-frequency area corresponds to the electron transfer control process, providing the electron transfer resistance (Ret). The straight part of the low-frequency area corresponds to the diffusion control

process [31], where the equivalentseries resistance (ESR) can be acquired. Figure 5 shows that the ESR almost had no change, and the semi-circle part of Co_3O_4/GCE in the high-frequency area was slightly larger than that of the GCE. Compared to GCE, the electron transfer resistance of $[Fe(CN)_6]^{3-/4-}$ was larger than that for Co_3O_4/GCE. This could be attributed to the fact that Co_3O_4 is a semiconductor material [27]. In contrast, it proved that the surface of GCE was successfully modified by Co_3O_4, and in accordance with the CV result, indicating that the Co_3O_4/GCE still had a good electrochemical catalytic behavior and electron-transfer rate, which shows good capacitance characteristics.

3.3 Effect of Operational Parameters

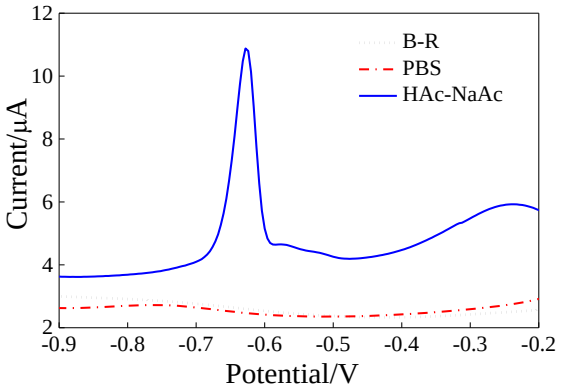

Figure 6. Effect of supporting electrolyte on the peak current of Pb^{2+} at Co_3O_4/GCE. Amplitude, 25 mV; frequency, 15 Hz; quite time: 2 s.

Co_3O_4/GCE exhibited different electrochemical reactions in different electrolytes. In this experiment, we studied the SWASV test of 3.5 μM Pb^{2+} with Co_3O_4/GCE in B-R buffer solution (pH=5.0), 0.1 M phosphate buffer solution (PBS, pH=5.8) and 0.1 M acetic acid-sodium acetate buffer solution (HAc-NaAc, pH=5.0). The test results showed that Pb^{2+} only responds in HAc-NaAc buffer solution (Figure 6). Therefore, HAc-NaAc solution was selected as the substrate solution for the detection of Pb^{2+} using Co_3O_4/GCE.

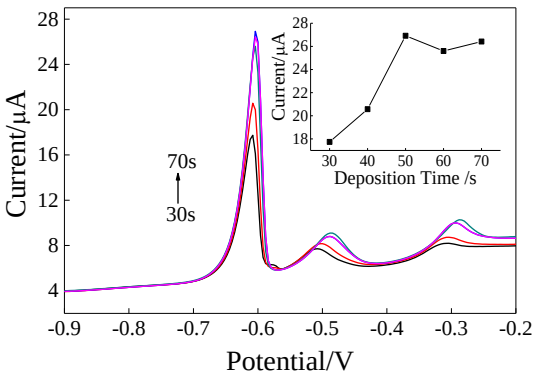

Figure 7. Effect of deposition time on the peak current of Pb^{2+} at Co_3O_4/GCE. Experimental parameters are the same as in Figure 6.

In the 0.1 M HAc-NaAc buffer solution (pH=5.0) in the presence of 3.5 μM Pb^{2+}, the SWASV response at different deposition times (30, 40, 50, 60 and 70 s) was compared. As shown in Figure 7, when the deposition time increased from 30 s to 50 s, the peak current kept increasing and reached the maximum value. However, after 50 s, with increasing deposition time, the dissolution peak showed slight change. This could be ascribed to the saturation of the available active sites on the electrode interface [2], thus the deposition time parameter was chosen as 50 s.

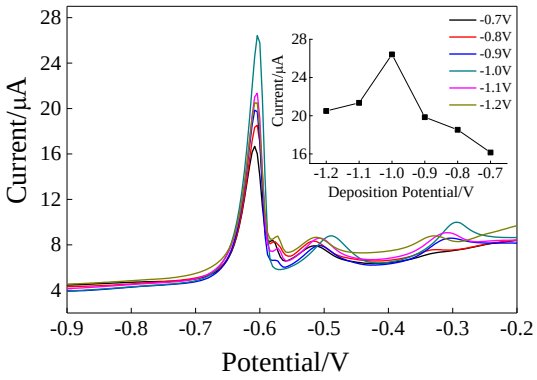

Figure 8. Effect of deposition potential on the peak current of Pb^{2+} at Co_3O_4/GCE. Experimental parameters are the same as in Figure 6.

Next, in the 0.1 M HAc-NaAc buffer solution (pH=5.0) in the presence of 3.5 μM Pb^{2+}, the effect of deposition potential on the peak current was studied in the range from –0.2 to 1.0 V. The test results are shown in Figure 8, indicating that the peak current shows an upward trend from –0.7 to –1.0 V. Therefore, the more negative deposition potential could easily result in a greater analytical signal [2]. As a result of increase in hydrogen evolution, the peak current started to drop from –1.0 to –1.2 V. Thus, the deposition potential parameter was set at –1.0 V.

3.4 Standard Curve and Detection Limit

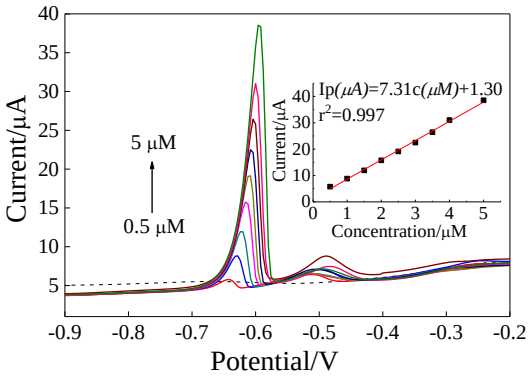

Figure 9. SWASV response toward Pb^{2+} on the Co_3O_4/GCE in the concentration range 0.5–5.0 μM by deposition for 50 s in 0.1 M HAc-NaAc buffer solution (pH=5.0). Inset is the linear calibration curve of Pb^{2+}. Deposition potential, –1.0 V; deposition time, 50 s; amplitude, 25 mV; frequency, 15 Hz; quite time, 2 s.

Under the optimized conditions, SWASV was used to determine Pb^{2+} on the Co_3O_4/GCE. Figure 9 shows the SWASV response of Pb^{2+} in the concentration range from 0.5 to 5.0 μM. The peak current increases proportionally with increasing concentration of Pb^{2+}. The linear equation was calculated as $Ip = 7.31c+1.30$ (*Ip* in μA, *c* in mol/L) and the correlation coefficient was 0.997. The limit of detection (LOD, calculated by the 3σ method) and the sensitivity were 1.18×10^{-8} M and 7.31 μA/μM, respectively. The results show that the Co_3O_4/GCE had excellent sensitivity for the detection of Pb^{2+}. Table 1 shows a comparison of the Co_3O_4/GCE and other fabricated electrodes. We noticed that the detection limit of Co_3O_4/GCE was slightly smaller than Fe_3O_4/GCE and Mn_3O_4-graphitic carbon/GCE. Furthermore, the linear range of Co_3O_4/GCE was larger than almost all the mentioned electrodes. Overall, this method is of great interest, as Co_3O_4 can be prepared by simple hydrothermal method without adding any surfactant, and the Co_3O_4/GCE has a sensitive response to Pb^{2+} in a wide detection range.

Table 1. Comparison of the Co_3O_4/GCE and other fabricated electrodes.

Modified electrode	Method	Linear range	LOD	Reference
MCN[A]-SPAN[B]/GCE	SWASV	0.005–0.08 μM	0.2 nM	17
MWNT[C]-Nafion/GCE	DPV	0.005–0.02 μM; 0.025–5 μM	1.0×10^{-9} M	3
Mn_3O_4-graphitic carbon/GCE	DPASV	0.02–0.68 μM	9.66×10^{-11} M	2
Fe-MOFs/PdPtNPs[D]-HP-BSA/GCE	chronoamperometry	0.005–1000 nM	2 pM	1
BiF[E]/SPCE[F]	SWASV	0.0005–0.5 μM	1.41×10^{-10} M	32
Fe_3O_4/GCE	SWASV	0.1–1.8 μM	0.0595 μM	28
Co_3O_4/GCE	SWASV	0.5–5 μM	1.18×10^{-8} M	this work

[A]MCN: Mesoporous Carbon Nitride
[B]SPAN: Self-Doped Polyaniline Nanofibers
[C]MWNT: Multiwalled Carbon Nanotube
[D]NPs: Nanoparticles
[E]BiF: Bismuth Films
[F]SPCE: Screen-printed Carbon Electrode

3.5 Repeatability and Interference Studies

Under the optimized condition, 2.5 μM Pb^{2+} was tested 10 times on Co_3O_4/GCE. The test results are shown in Figure 10, indicating that the peak shape did not change and the test curves almost

overlapped. The standard deviation of the peak current value in Table 2 was calculated as 1.96%, indicating that the Co_3O_4/GCE has a good stability.

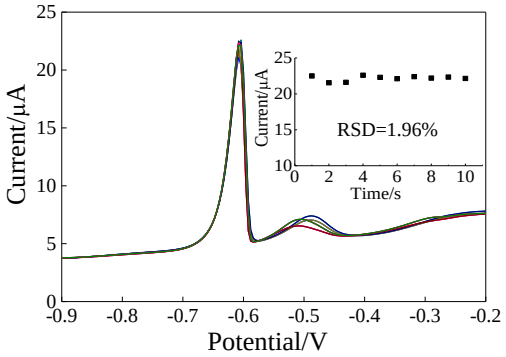

Figure 10. Repeatability measurements of 2.5μM Pb^{2+} on the Co_3O_4/GCE in 0.1 M HAc-NaAc (pH=5.0). Inset is the repeatability of the Co_3O_4/GCEat ten parallel measurements forPb^{2+}. All other parameters are the same asin Figure 9.

In the 0.1 M HAc-NaAc buffer solution (pH=5.0), the interference to the detection of Pb^{2+} was also investigated with two heavy metal ions, Cd^{2+} and Hg^{2+}. The test results are shown in Figure 11. After adding 4.5 μM Cd^{2+} and 1.5 μM Hg^{2+}, the concentration of Pb^{2+} was determined by Co_3O_4/GCE. It was found that the dissolution peak of Cd^{2+} and Hg^{2+} appeared at approximately –0.85 V and 0.1 V, respectively. The dissolution peak of Pb^{2+} shifted slightly to the right and the peak current value was almost constant, indicating that Cd^{2+} and Hg^{2+} did not interfere with the detection of Pb^{2+}.

Table 2. The standard deviation of peak current value. Pb^{2+} was detected with Co_3O_4/GCE, and the measurement was repeated10 times.

Time	1	2	3	4	5	6	7	8	9	10	RSD(%)
Peak current/μA	22.5	21.55	21.11	22.6	22.3	22.11	22.4	22.2	22.34	22.15	1.96%

3.6 Real Sample Analysis

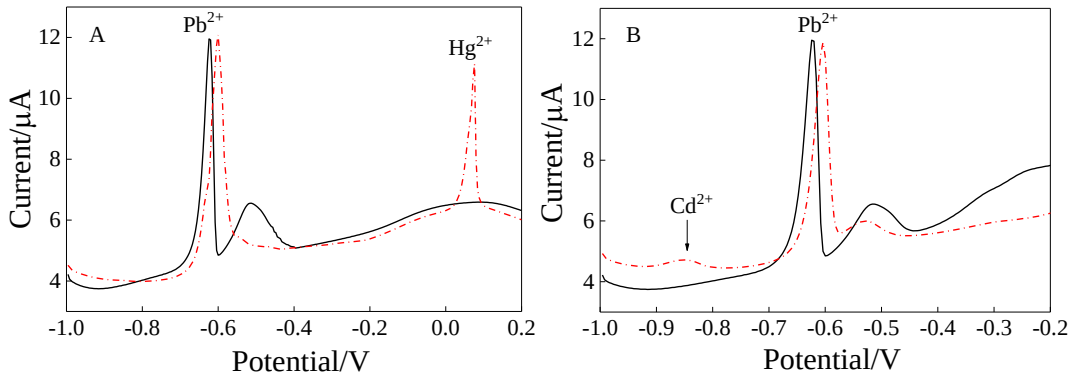

Figure 11. Electrochemical detection of 1.5 μM Pb^{2+} with Co_3O_4/GCE and its interference with (A) 1.5 μM Hg^{2+} and (B) 4.5 μM Cd^{2+}. All other parameters are the same as in Figure 9.

The spike and recovery experiment was investigated to determine the concentration of Pb^{2+} in local tap water samples. Since the concentration of Pb^{2+} was unknown in the tap water samples, the experiment was carried out via adding known concentrations of Pb^{2+}. As shown in Table 3, the calculated recovery rate was between 98.00% and 102.00%, revealing that Pb^{2+} did not exist in the tap water samples. As a result, the prepared Co_3O_4/GCE could serve as a practical and reliable tool for the detection of Pb^{2+}.

Table 3. Recovery results for Pb^{2+} with modified electrodes in tap water

Sample	Content (μM)	Added (μM)	Found (μM)	Recovery(%)
1	0.50	0.50	1.01	102.00%
2	1.00	0.50	1.48	98.00%
3	1.50	0.50	1.98	98.67%

4. CONCLUSIONS

In this study, Co_3O_4/GCE was prepared and used to determine trace lead(II) by SWASV. The Co_3O_4/GCE was able to provide larger active areas for Pb^{2+}. The effects of supporting electrolytes, deposition time, and deposition potential were investigated to improve the electrode sensitivity and anti-interference ability. In future, Co_3O_4-based hexagon microsheet-stacked structure will provide more ways to develop new electrodes for the determination of heavy metals.

ACKNOWLEDGMENTS
This research did not receive any specific funding.

NOTES
The authors declare no conflicts of interest.

References

1. Y. Yu, C. Yu, Y. Niu, J. Chen, Y. Zhao, Y. Zhang, R. Gao, J. He, *Biosens. Bioelectron.*, 229 (2017) 297.
2. P.S. Adarakatti, V.K. Gangaiah, C.E. Banks, A. Siddaramanna, *J. Mater. Sci.*, 53 (2018) 4961.
3. Q. Xu, N. Liu, J Zhu, *Chin. J. Chem.*, 23 (2005) 1510.
4. J. M. Jian, Y. Y. Liu, Y. L. Zhang, X. S. Guo, Q Cai, *Sens.*, 13 (2013) 13063.
5. T.M.D. Oliveira, J.A. Peres, M.L. Felsner, K.C. Justi, *Food Chem.*, 29 (2017) 721.
6. W. Zhong, T. Ren, L. Zhao, *J. Food Drug Anal.*, 24 (2016) 46.
7. H. Ciftci, M.M. Temuz, E. Ciftci, *J. AOAC Int.*, 96 (2013) 875.
8. A. Zou, Y. Liu, M. Chen, J. Wang, *Chin. J. Anal. Chem.*, 36 (2008) 162.
9. J. Xue, S. Gong, X. Wang, Y. Fan, X. Li, *Anal. Lett.*, 45 (2012) 2257.
10. I. Rapp, C. Schlosser, D. Rusiecka, M. Gledhill, E.P. Achterberg, *Anal. Chim. Acta*, 976 (2017) 1.
11. C. Y. Tai, S. J. Jiang, A. C. Sahayam, *Food Chem.*, 192 (2016) 274.
12. R. P. Lamsal, D. Beauchemin, Anal.*Chim. Acta*, 867 (2015) 9.

13. H. Lu, S. Mou, Y. Yan, S Tong, JM Riviello, *J. Chromatogr. A*, 800 (1998) 247.
14. R. J. Vancott, B. J. Mcdonald, A. G. Seelos,*Nucl. Instrum. Methods Phys. Res.*, 422 (1999) 801.
15. M. G. Nejad, H Faraji, A Moghimi, *Bull. Environ. Contam. Toxicol.*, 98 (2017) 546.
16. M. Iqbal, A. Saeed, S.I. Zafar, *J. Hazard. Mater.*, 164 (2009) 161.
17. C. Zhang, Y. Zhou, L. Tang, G. Zeng, J. Zhang, B. Peng, X. Xie, C. Lai, B. Long, J. Zhu, *Nanomaterials*, 6 (2016) 7.
18. J. Lv, X. He, X. Zeng, Z. Zhang, *Chin. J. Chem.*, 21 (2003) 687.
19. K. Pourzare, S. Farhadi, Y. Mansourpanah, *ActaChim. Slov.*, 64 (2017) 945.
20. X. Lang, H. Fu, C. Hou, G. Han, P. Yang, Y. Liu, Q. Jiang, *Nat. Commun.*, 4 (2013) 2169.
21. F. Liu, B. Zhang, H. Su, H. Zhang, L. Zhang, W. Yang, *Nanotechnol.*, 27 (2016) 355603.
22. C. Shin, J. Manuel, D.S. Kim, H.S. Ryu, H.J. Ahn, J.H. Ahn, *Nanoscale Res. Lett.*, 7 (2012) 73.
23. L. Xie, K. Li, G. Sun, Z. Hu, C. Lv, J. Wang, C. Zhang, *J. Solid State Electrochem.*, 17 (2013) 55.
24. P. Balaya, *Energy Environ. Sci.*, 1 (2008) 645.
25. Y. Liu, C. Mi, L. Su, X. Zhang, *Electrochim. Acta*, 53 (2008) 2507.
26. Y. Zhang, Y. Chen, T. Wang, J. Zhou, Y. Zhao, *Microporous Mesoporous Mater.*, 114 (2008) 257.
27. Z. Wen, L. Zhu, W. Mei, Y. Li, L. Hu, L. Sun, W Wan, Z Ye, *J. Mater. Chem. A*, 1 (2013) 7511.
28. W. Li, X. Yao, Z. Guo, J. Liu, X. Huang, *J. Electroanal. Chem.*, 749 (2015) 75.
29. K. Rechendorff, M.B. Hovgaard, M. Foss, V.P. Zhdanov, F. Besenbacher, *Langmuir*, 22 (2006) 10885.
30. K. Thangavelu, K. Parameswari, K. Kuppusamy, Y. Haldorai, *Mater. Lett.*, 65 (2011) 1482.
31. Y. Sun, W. Chen, W. Li, T. Jiang, J. Liu, Z. Liu, *J. Electroanal. Chem.*, 714-715 (2014) 97.
32. K. Tyszczuk-Rotko, K. Domańska, *J. Electrochem. Soc.*, 164 (2017) H537.